

NOTE**Uptake of porewater phosphate by REY-rich mud
in the western North Pacific Ocean**AKIRA IJIRI,^{1,2*} KEI OKAMURA,³ JUNICHIRO OHTA,^{4,5,6} YOSHIRO NISHIO,³ YOHEI HAMADA,^{1,7}
KOICHI IJIMA² and FUMIO INAGAKI^{1,2,7}¹Kochi Institute for Core Sample Research, Japan Agency for Marine-Earth Science and Technology (JAMSTEC),
Nankoku, Kochi 783-8502, Japan²Research and Development Center for Submarine Resources, JAMSTEC, Yokosuka, Kanagawa 237-0061, Japan³Center for Advanced Marine Core Research, Kochi University, Nankoku, Kochi 783-8502, Japan⁴Ocean Resources Research Center for Next Generation, Chiba Institute of Technology, Chiba 275-0016, Japan⁵Department of Solid Earth Geochemistry, JAMSTEC, Yokosuka, Kanagawa 237-0061, Japan⁶Frontier Research Center for Energy and Resources, The University of Tokyo, Tokyo 113-8656, Japan⁷Research and Development Center for Ocean Drilling Science, JAMSTEC, Yokohama, Kanagawa 236-0001, Japan

(Received September 16, 2017; Accepted January 26, 2018)

Deep-sea mud extremely enriched in rare-earth elements and yttrium (together called REY) has been discovered around Minamitorishima Island, in the western North Pacific. The REY-rich mud was previously observed to contain abundant phillipsite and biogenic calcium phosphate. We analyzed the chemical compositions of porewater in a sediment core containing REY-rich mud and observed a decrease of dissolved phosphate (PO_4^{3-}) from $\sim 1 \mu\text{M}$ to $\sim 0.5 \mu\text{M}$ around the REY-rich mud layer. The presence of dissolved nitrate + nitrite throughout the cored depth indicated oxic sediment conditions. In the REY-rich mud, PO_4^{3-} was presumed to be adsorbed onto the surfaces of minerals such as phillipsite. Our results support that oxic pelagic clay containing phillipsite can be a sink for PO_4^{3-} . Concentrations of REY in porewater were below the detection limit.

Keywords: phosphate, rare-earth elements, nitrate, porewater, Minamitorishima Island

INTRODUCTION

Deep-sea mud extremely enriched in rare-earth elements (REEs) and yttrium (together called REY) has been discovered in the Japanese Exclusive Economic Zone around Minamitorishima Island in the western North Pacific Ocean (Iijima *et al.*, 2016). It was showed that biogenic phosphate is the main host phase of REY in the REY-enriched deep-sea sediments around Minamitorishima (Kashiwabara *et al.*, 2014). To investigate the mechanism of REY uptakes by biogenic calcium phosphate, we analyzed PO_4^{3-} , Ca^{2+} , and REY dissolved in porewater in the REY-rich sediments. The high REE concentrations in fish debris are found during early diagenesis at sediment-water interface and Nd isotopic composition of fish debris faithfully record the Nd isotopic composition of bottom water (e.g., Martin and Scher,

2004). Therefore, the adsorption of REEs from porewater to apatite in the sediment column would be insignificant. However, the behavior of porewater REEs in the sediment containing the REY-rich mud is unknown. It is important for our understanding of the REY accumulation process to ascertain whether REY in porewater is accumulated in situ in biogenic apatite in sediments, or released from the REY-rich sediment. Furthermore, it is necessary to know the redox condition of the sediments to evaluate whether authigenic apatite may have precipitated and to infer the behavior of REY in the sediments. Here, we present the chemical characteristics of porewater in the REY-enriched deep-sea sediments.

MATERIALS AND METHODS

We studied piston core PC04 ($21^\circ 56.11' \text{N}$, $152^\circ 39.51' \text{E}$; water depth 5720 m; core length 12.73 m), in which highly REY-rich mud was discovered. PC04 was retrieved from the Japanese Exclusive Economic Zone around Minamitorishima Island in the western North Pacific Ocean in January 2013 during cruise KR13-02 of R/V

*Corresponding author (e-mail: ijiri@jamstec.go.jp)

Copyright © 2018 by The Geochemical Society of Japan.

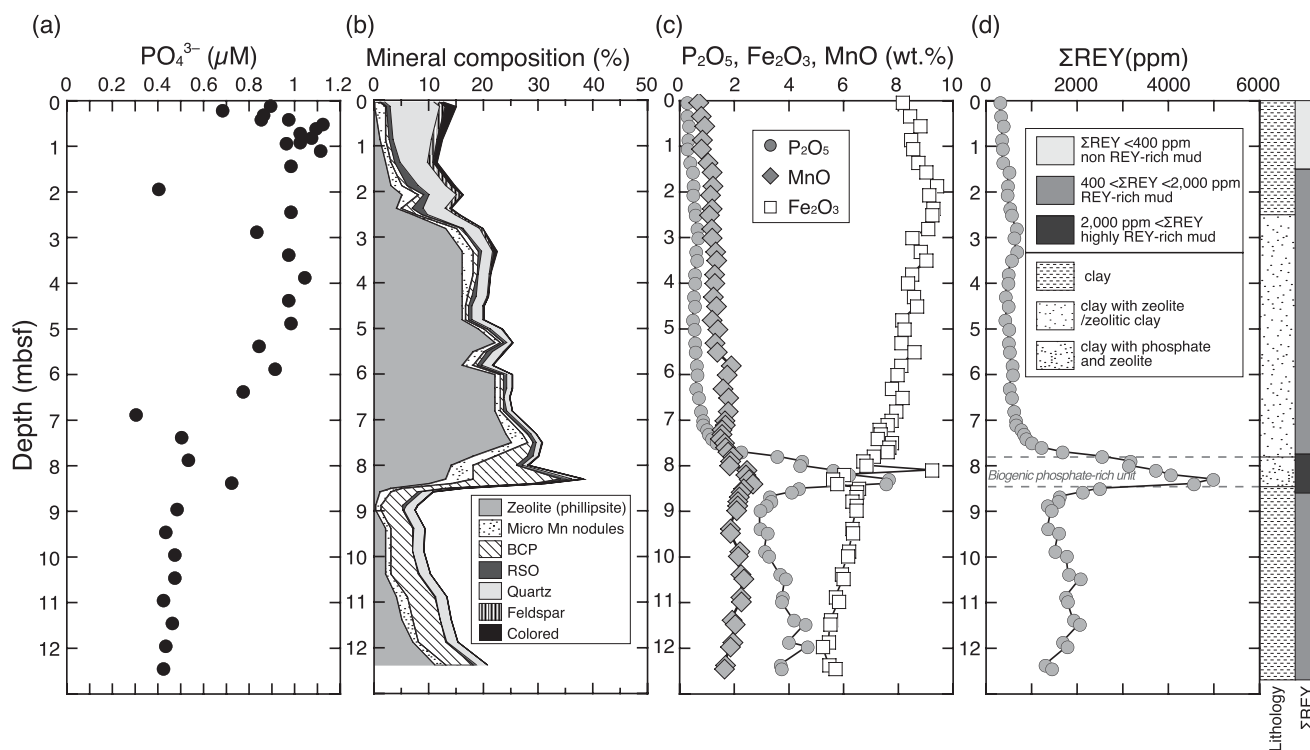


Fig. 1. Depth profiles of (a) dissolved PO_4^{3-} in porewater, (b) mineral compositions, (c) P_2O_5 , Fe_2O_3 , MnO , and (d) ΣREY contents with lithology in the sediments of PC04 and PL04. BCP and RSO in (b) are biogenic Ca phosphate and red-brown to yellow-brown semiopaque oxide, respectively. Chemical composition data of the sediments and the lithology are from Iijima *et al.* (2016). Lithology was modified from Iijima *et al.* (2016) and Ohta *et al.* (2016).

Kairei (Iijima *et al.*, 2016). We studied the surface sediment in gravity core PL04 (core length 1.28 m), which was retrieved by a gravity corer attached to the tripping arm of the piston corer. REY-rich sediment ($\Sigma\text{REY} > 1000$ ppm) was observed deeper than 7.5 m below seafloor (mbsf) at the PC04 core site (Iijima *et al.*, 2016; Fig. 1). Within the REY-rich sediments, an extremely REY-enriched layer ($\Sigma\text{REY} > 4000$ ppm) was observed at 8.2–8.4 mbsf. The vertical profile of P_2O_5 in core PC04 is similar to that of ΣREY (Iijima *et al.*, 2016). The vertical profile of P_2O_5 generally represents the content of biogenic calcium phosphate such as fish teeth or bone debris, and the high P_2O_5 concentration is indicative of abundant biogenic calcium phosphate (Iijima *et al.*, 2016). Porewater samples were extracted onboard with a Rhizon sampler (Dickens *et al.*, 2007). Immediately after its recovery, core PC04 was cut into 1 m slices, and then 4-mm-diameter holes were drilled through the core liner, at 50 cm intervals in PC04 and at 10 cm intervals in PL04. To extract the porewater via these holes, the porous tube of a Rhizon sampler (a diameter of 2.5 mm; a mean pore size of $0.15 \mu\text{m}$) was inserted into the sediment and buried in the sediment through the hole. The core samples were stored in a refrigerator at 4°C during the extraction

of porewater.

The extracted porewater was filtered through $0.2 \mu\text{m}$ Millipore PTFE filters, and subsamples (about 5 ml) from each were stored at -20°C in precombusted 10 ml glass vials, each with a Teflon-coated septum and a screw cap, for later measurement of dissolved phosphate (PO_4^{3-}), nitrate + nitrite ($\text{NO}_3^- + \text{NO}_2^-$), and silicate (SiO_2). The remaining porewater samples were stored in polypropylene bottles under refrigeration at 4°C until measurement of the major and trace elements, including REY.

Dissolved $\text{NO}_3^- + \text{NO}_2^-$, PO_4^{3-} , and SiO_2 concentrations in porewater were analyzed with an autoanalyzer (Autoanalyzer-II, BL-TEC). The analytical precisions were $\pm 1\%$ at a concentration of $1 \mu\text{mol L}^{-1}$ for NO_3^- and SiO_2 , and $\pm 2\%$ at a concentration of $0.4 \mu\text{mol L}^{-1}$ for PO_4^{3-} .

The concentrations of the major cations Na, Mg, K, and Ca in porewater were determined with an ion chromatograph (ICS-2000, Dionex). Analytical precision was estimated to be within 1% from repeated measurements of the same samples.

Trace elements, including REEs, in porewater were determined by inductively coupled plasma mass

Table 1. Phosphate, nitrate + nitrite, silica, and major cations in porewater samples extracted from PC04 and PL04

| Sample | Depth (cmbsf) | PO ₄ (μM) | NO ₃ + NO ₂ (μM) | Si (μM) | Na (mM) | Mg (mM) | Ca (mM) | K (mM) |
|-----------------|---------------|----------------------|--|---------|---------|---------|---------|--------|
| PL04 Sec1 10cm | 10 | 0.89 | 38.0 | 252 | 478 | 52.0 | 10.2 | 11.7 |
| PL04 Sec1 20cm | 20 | 0.68 | 40.1 | 255 | 473 | 51.1 | 10.1 | 11.6 |
| PL04 Sec1 30cm | 30 | 0.86 | 38.6 | 262 | 470 | 50.7 | 10.0 | 11.5 |
| PL04 Sec1 40cm | 40 | 0.97 | 40.2 | 264 | 486 | 52.6 | 10.3 | 11.8 |
| PL04 Sec1 50cm | 50 | 1.12 | 40.1 | 274 | 464 | 50.2 | 9.9 | 11.3 |
| PL04 Sec1 60cm | 60 | 1.09 | 41.5 | 284 | 482 | 52.0 | 10.2 | 11.7 |
| PL04 Sec1 70cm | 70 | 1.02 | 40.1 | 264 | — | — | — | — |
| PL04 Sec1 80cm | 80 | 1.07 | 40.7 | 272 | 484 | 52.5 | 10.3 | 11.8 |
| PL04 Sec1 90cm | 90 | 1.02 | 41.6 | 264 | — | — | — | — |
| PL04 Sec2 10cm | 108.5 | 1.11 | 41.8 | 289 | 464 | 50.0 | 9.8 | 11.3 |
| PC04 Sec8 40cm | 40 | 0.85 | 39.2 | 314 | 486 | 52.3 | 10.3 | 12.1 |
| PC04 Sec9 40cm | 92 | 0.96 | 38.5 | 305 | 491 | 52.9 | 10.6 | 12.4 |
| PC04 Sec9 90cm | 142 | 0.98 | 39.5 | 307 | 499 | 53.9 | 10.7 | 12.6 |
| PC04 Sec10 40cm | 192.5 | 0.40 | 41.4 | 303 | 476 | 51.2 | 10.1 | 11.7 |
| PC04 Sec10 90cm | 242.5 | 0.98 | 42.0 | 300 | 479 | 51.9 | 10.3 | 11.6 |
| PC04 Sec11 40cm | 286.5 | 0.83 | 43.5 | 269 | — | — | — | — |
| PC04 Sec11 90cm | 336.5 | 0.97 | 41.3 | 265 | 478 | 52.2 | 10.2 | 11.5 |
| PC04 Sec12 40cm | 386 | 1.04 | 44.1 | 272 | 487 | 52.9 | 10.3 | 11.9 |
| PC04 Sec12 90cm | 436 | 0.97 | 45.3 | 243 | 479 | 52.2 | 10.2 | 11.7 |
| PC04 Sec13 40cm | 486.5 | 0.98 | 44.4 | 274 | 490 | 53.1 | 10.4 | 12.1 |
| PC04 Sec13 90cm | 536.5 | 0.84 | 44.3 | 265 | 488 | 53.2 | 10.4 | 11.7 |
| PC04 Sec14 40cm | 586.5 | 0.91 | 43.9 | 266 | 478 | 51.7 | 10.2 | 11.8 |
| PC04 Sec14 90cm | 636.5 | 0.77 | 44.6 | 244 | 468 | 51.3 | 10.0 | 11.0 |
| PC04 Sec15 40cm | 686.5 | 0.30 | 47.2 | 259 | 492 | 53.2 | 10.4 | 11.9 |
| PC04 Sec15 90cm | 736.5 | 0.50 | 46.6 | 259 | 485 | 52.5 | 10.2 | 11.8 |
| PC04 Sec16 40cm | 786 | 0.53 | 47.1 | 266 | 501 | 53.8 | 10.4 | 12.5 |
| PC04 Sec16 90cm | 836 | 0.72 | 49.9 | 295 | — | — | — | — |
| PC04 Sec17 40cm | 894 | 0.48 | 46.1 | 241 | — | — | — | — |
| PC04 Sec17 90cm | 944 | 0.43 | 48.3 | 251 | 497 | 54.6 | 10.5 | 11.5 |
| PC04 Sec18 40cm | 1044 | 0.47 | 48.0 | 244 | 492 | 54.1 | 10.4 | 11.4 |
| PC04 Sec18 90cm | 994 | 0.47 | 46.6 | 247 | — | — | — | — |
| PC04 Sec19 40cm | 1093.5 | 0.42 | 48.0 | 272 | — | — | — | — |
| PC04 Sec19 90cm | 1143.5 | 0.46 | 47.3 | 283 | — | — | — | — |
| PC04 Sec20 40cm | 1193.5 | 0.43 | 48.4 | 282 | 467 | 50.6 | 9.6 | 12.3 |
| PC04 Sec20 90cm | 1243.5 | 0.42 | 48.0 | 271 | 493 | 54.1 | 10.2 | 12.6 |

—: no sample.

spectrometry (ICP-MS, ELAN-DRC II, PerkinElmer) using a sample solution diluted by a factor of 1000 and containing an internal standard of indium. The uncertainties of the concentrations were within $\pm 3\%$. The detection limits of REEs are listed in supplementary Table S1 that were estimated from the reproducibility (3σ) of 2% HNO₃ ($n = 10$) used as a blank solution.

The mineral compositions were semi-quantitatively estimated by the observation under a polarizing microscope following the protocols of the International Ocean Discovery Program (IODP) (Ohta *et al.*, 2016). We identified the mineral compositions for the grains larger than 4 μm, and categorized grains that were smaller than 4 μm as clay-sized particles because mineral identification of these grains is difficult under an optical microscope.

RESULTS AND DISCUSSION

The PO₄³⁻ concentration increased slightly, from about 0.9 μM near the seafloor to 1.1 μM at 1 m below the seafloor (mbsf); between 1 and 6 mbsf, it was ~ 1 μM; and from 6 to 7.4 mbsf, it decreased to 0.5 μM. Below 7.4 mbsf, the PO₄³⁻ concentration remained approximately constant at 0.4–0.5 μM (Fig. 1a, Table 1) without the local increase at 8.4 mbsf. The PO₄³⁻ concentration near the sediment surface was lower than the concentration in the modern bottom water near the core site (~ 2.4 μM; Talley, 2007), which suggests that PO₄³⁻ in the bottom water is taken up by the sediments. The low PO₄³⁻ concentrations were observed at the depths of ~ 2 mbsf and ~ 7 mbsf, suggesting the local uptake of PO₄³⁻ at the

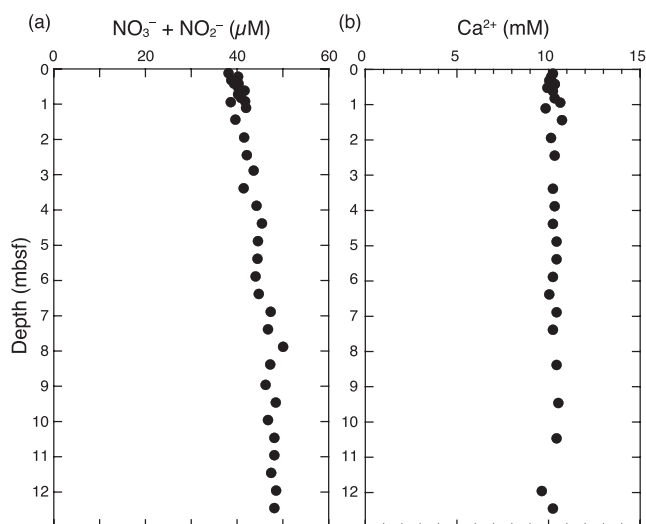


Fig. 2. Depth profiles of (a) NO_3^- and (b) Ca^{2+} dissolved in porewater of PC04 and PL04.

depths.

Dissolved $\text{NO}_3^- + \text{NO}_2^-$ increased slightly from $\sim 38 \mu\text{M}$ near the surface to $\sim 48 \mu\text{M}$ at the core bottom (Fig. 2a). The $\text{NO}_3^- + \text{NO}_2^-$ concentration near the surface was slightly higher than that in the modern bottom water ($\sim 34 \mu\text{M}$; Talley, 2007). Because dissolved NO_3^- is produced in sediment by aerobic degradation and subsequent nitrification of ammonium regenerated from buried organic matter, the slight increase by $\sim 10 \mu\text{M}$ from near the surface to the bottom is a strong indication of the presence of dissolved O_2 and, thus, oxic conditions, throughout the cored depth (D'Hondt *et al.*, 2015, Fig. 2a). In the ultra-oligotrophic South Pacific Gyre, dissolved NO_3^- and O_2 concentrations in porewater closely match the Redfield $\text{NO}_3^-:\text{O}_2$ ratio (D'Hondt *et al.*, 2015). From the O_2 concentration of the bottom water near the core site ($178 \mu\text{M}$; Talley, 2007) and the Redfield $\text{NO}_3^-:\text{O}_2$ ratio (16:–170; D'Hondt *et al.*, 2015), the O_2 concentration in the bottom sediment of the core (12.4 mbsf) can be estimated to be $111 \mu\text{mol}$. The aerobic degradation of organic matter should cause increases of PO_4^{3-} and NO_3^- in accordance with the Redfield N:P ratio (15:1). The fact that the PO_4^{3-} concentration did not increase with $\text{NO}_3^- + \text{NO}_2^-$ (Figs. 1a and 2a) indicates that PO_4^{3-} is taken up by the sediments. In addition, because the sediments were oxic, the decrease of PO_4^{3-} in the REY-rich mud cannot be explained by the precipitation of the authigenic minerals such as apatite ($\text{Ca}_5(\text{PO}_4)_3(\text{OH},\text{F})$) or vivinite ($\text{Fe}_3(\text{PO}_4)_2 \cdot 8\text{H}_2\text{O}$, which occurs only under anoxic conditions (Berner, 1974). Additionally, no uptake of Ca due to precipitation of authigenic apatite could be recognized because dissolved Ca^{2+} was constant at $10.2 \pm 0.2 \text{ mM}$

(i.e., close to the seawater concentration of 10.3 mM) throughout the cored depth (Fig. 2b). Under oxic conditions, PO_4^{3-} is adsorbed on ferric oxides, clay, aluminum oxides, and, possibly, Mn oxides (Ruttenberg and Berner, 1993). Among these potential adsorbents, the amounts of Fe-Mn oxides were only very minor in the highly REY-rich mud (Ohta *et al.*, 2016), and the Fe content of the sediment decreased with increasing depth below 3 mbsf (Fig. 1c; Iijima *et al.*, 2016). Therefore, ferric oxides were not the main adsorbent of PO_4^{3-} in the REY-rich mud. However, Mn oxide cannot be ruled out as a potential adsorbent of PO_4^{3-} because of the relatively high Mn content (Fig. 1c; Iijima *et al.*, 2016) below 7 mbsf where the PO_4^{3-} concentrations are generally low at $0.4\text{--}0.5 \mu\text{M}$. Based on the vertical profiles of mineral compositions (Fig. 1b, Table 2), we assume that the most plausible adsorbent of PO_4^{3-} is phillipsite. The content of phillipsite increased from $\sim 5\%$ at 2.4 mbsf to 16% at 3.3 m. Below 4.8 mbsf, the content increased to 25% at 7.5 mbsf with local peak at 5.3 mbsf. The increase of phillipsite content between 4.8 mbsf and 7.5 mbsf is consistent with the decrease of PO_4^{3-} . Below the 7.5 mbsf, the phillipsite content decreased below 1% at 8.9 mbsf, and then increased to 11% at core bottom. Interestingly, the local decreases of PO_4^{3-} at ~ 2 mbsf and ~ 8 mbsf are near the peaks of the phillipsite content, and local increase of PO_4^{3-} at 8.4 mbsf is close to the depth interval where phillipsite content was low.

A decrease of PO_4^{3-} in porewater has been observed in similar pelagic marine sediments, mainly composed of clay and containing phillipsite, in the ultra-oligotrophic South Pacific Gyre (D'Hondt *et al.*, 2015) where O_2 penetrated from the seafloor to the sedimentary basement. Phillipsite is an alteration product of volcanic glass, and it is abundant in most Pacific Ocean seafloor sediments (Glaccum and Boström, 1976). Under oxic conditions, pelagic clay sediments containing phillipsite are expected to be an important sink of PO_4^{3-} found in porewater and therefore seawater. Our results confirm that such sediments are a sink for porewater PO_4^{3-} .

The REE concentrations of all porewaters analyzed in this study were significantly lower than the detection limits (Supplementary Table S1). Even if the mud is enriched in REEs, the porewater in muds, therefore, does not contain the REEs exceeding the μM level.

Acknowledgments—We acknowledge the officers, crew, and shipboard scientific party of the KR13-02 cruise of R/V *Karei* for sample retrieval and technical support. This work was supported in part by the Japan Society for the Promotion of Science through a Grant-in-Aid for Science Research 17H01871. The authors are grateful to A. Imajyo and M. Hatta for technical assistance.

Table 2. Mineral compositions in PC04

| Sample | Depth (cmbsf) | Quartz (%) | Feldspar (%) | Zeolite (phillipsite) (%) | BCP (%) | RSO (%) | micro Mn nodule (%) | Colored minerals (%) |
|-------------------|---------------|------------|--------------|---------------------------|---------|---------|---------------------|----------------------|
| PC04-1 2–4 cm | 3 | 9 | 1 | — | 0 | 0.7 | 1 | 0.7 |
| PC04-1 12–14 cm | 13 | 9 | 1 | — | 0 | 0.7 | 2 | 2 |
| PC04-2 32–24 cm | 85 | 7 | 1 | 1 | 1 | 0.7 | 1 | 1 |
| PC04-2 82–84 cm | 135 | 5 | 1 | 2 | 1 | 1 | 1 | 0.7 |
| PC04-3 32–34 cm | 186 | 5 | 1 | 3 | 1 | 2 | 2 | 0.7 |
| PC04-3 52–54 cm | 205.5 | 5 | 1 | 5 | 1 | 1 | 3 | 0.2 |
| PC04-3 82–84 cm | 235.5 | 4 | 0.9 | 4 | 2 | 2 | 0.9 | 0.2 |
| PC04-4 2–4 cm | 249.5 | 5 | 0.7 | 7 | 1 | 1 | 0.7 | 0.2 |
| PC04-4 32–34 cm | 280 | 3 | 0.6 | 13 | 1 | 0.2 | 2 | — |
| PC04-4 82–84 cm | 329.5 | 2 | 0.2 | 16 | 1 | 0.6 | 2 | 0.6 |
| PC04-5 32–34 cm | 380 | 2 | 0.2 | 16 | 1 | 0.2 | 2 | — |
| PC04-5 82–84 cm | 429 | 2 | 0.2 | 16 | 1 | 0.8 | 1 | — |
| PC04-6 2–4 cm | 449.5 | 2 | 0.2 | 16 | 1 | 0.6 | 0.6 | — |
| PC04-6 32–34 cm | 480 | 2 | 0.2 | 16 | 1 | 0.6 | 0.6 | — |
| PC04-6 52–54 cm | 499.5 | 2 | 0.2 | 19 | 1 | 0.6 | 1 | — |
| PC04-6 82–84 cm | 529.5 | 1 | 0.1 | 22 | 1 | 0.6 | 1 | — |
| PC04-7 2–4 cm | 549.5 | 2 | 0.2 | 18 | 1 | 1 | 2 | — |
| PC04-7 32–34 cm | 580 | 2 | — | 16 | 1 | 0.8 | 2 | — |
| PC04-7 52–54 cm | 599.5 | 1 | — | 22 | 1 | 0.6 | 1 | — |
| PC04-7 82–84 cm | 629.5 | 1 | — | 22 | 1 | 0.6 | 1 | — |
| PC04-8 2–4 cm | 649.5 | 1 | — | 22 | 1 | 0.1 | 1 | — |
| PC04-8 32–34 cm | 680 | 1 | — | 22 | 1 | 0.6 | 1 | — |
| PC04-8 82–84 cm | 729.5 | 1 | — | 24 | 1 | 0.6 | 3 | — |
| PC04-9 2–4 cm | 749 | 1 | — | 25 | 1 | 0.6 | 3 | 0.1 |
| PC04-9 32–34 cm | 779 | 1 | — | 18 | 6 | 1 | 4 | — |
| PC04-9 52–54 cm | 799 | 1 | 0.1 | 14 | 8 | 1 | 4 | — |
| PC04-9 82–84 cm | 829 | 2 | 0.2 | 13 | 16 | 2 | 5 | — |
| PC04-9 92–94 cm | 839 | 1 | 0.1 | 10 | 15 | 1 | 4 | — |
| PC04-9 102–104 cm | 849 | 2 | 0.2 | 3 | 8 | 1 | 2 | — |
| PC04-10 2–4 cm | 857 | 2 | — | 1 | 5 | 0.7 | 2 | — |
| PC04-10 32–34 cm | 887 | 2 | — | 0 | 4 | 0.7 | 1 | — |
| PC04-10 42–44 cm | 897 | 2 | — | 0 | 4 | 0.2 | 1 | — |
| PC04-10 82–84 cm | 937 | 2 | — | 2 | 4 | 0.2 | 1 | — |
| PC04-11 32–34 cm | 987 | 2 | — | 2 | 4 | — | 1 | — |
| PC04-11 82–84 cm | 1037 | 2 | — | 2 | 5 | 0.2 | 1 | — |
| PC04-12 32–34 cm | 1087 | 2 | — | 4 | 5 | 0.2 | 2 | — |
| PC04-12 82–84 cm | 1136.5 | 2 | — | 5 | 5 | — | 2 | — |
| PC04-13 32–34 cm | 1186 | 2 | — | 7 | 5 | 0.2 | 1 | — |
| PC04-13 82–84 cm | 1236 | 2 | — | 11 | 5 | 0.6 | 2 | — |

BCP: biogenic Ca phosphate, RSO: red-brown to yellow-brown semiopaque oxide.
 —: not detected.

REFERENCES

Berner, R. A. (1974) Kinetic models for the early diagenesis of nitrogen, sulfur, phosphorous, and silicon in anoxic marine sediments. *The Sea* 5 (Goldberg, E. D., ed.), 427–450, Wiley, New York.
 D'Hondt, S., Inagaki, F., Zarikian, C. A., Abrams, L. J., Dubois,

N., Engelhardt, T., Evans, H., Ferdelman, T., Gribsholt, B., Harris, R. N., Hoppie, B. W., Hyun, J. H., Kallmeyer, J., Kim, J., Lynch, J. E., McKinley, C. C., Mitsunobu, S., Morono, Y., Murray, R. W., Pockalny, R., Sauvage, J., Shimono, T., Shiraishi, F., Smith, D. C., Smith-Duque, C. E., Spivack, A. J., Steinsbu, B. O., Suzuki, Y., Szpak, M., Toffin, L., Uramoto, G., Yamaguchi, Y. T., Zhang, G. L.,

- Zhang, X. H. and Ziebis, W. (2015) Presence of oxygen and aerobic communities from sea floor to basement in deep-sea sediments. *Nat. Geosci.* **8**, 299–304.
- Dickens, G. R., Koelling, M., Smith, D. C., Schnieders, L. and the IODP Expedition 302 Scientists (2007) Rhizon Sampling of Pore Waters on Scientific Drilling Expeditions: An Example from the IODP Expedition 302, Arctic Coring Expedition (ACEX). *Sci. Dril.* **4**, 22–25; <https://doi.org/10.2204/iodp.sd.4.08.2007>
- Glaccum, R. and Boström, K. (1976) (Na,K)-phillipsite: its stability conditions and geochemical role in the deep sea. *Mar. Geol.* **21**, 47–58.
- Iijima, K., Yasukawa, K., Fujinaga, K., Nakamura, K., Machida, S., Takaya, Y., Ohta, J., Haraguchi, S., Nishio, Y., Usui, Y., Nozaki, T., Yamazaki, T., Ichiyama, Y., Ijiri, A., Inagaki, F., Machiyama, H., Suzuki, K., Kato, Y. and KR13-02 Cruise Members (2016) Discovery of extremely REY-rich mud in the western North Pacific Ocean. *Geochem. J.* **50**, 557–573.
- Kashiwabara, T., Toda, R., Kato, Y., Fujinaga, K., Takahashi, Y. and Honma, T. (2014) Determination of host phase of lanthanum in deep-sea REY-rich mud by XAFS and m-XRF using high-energy synchrotron radiation. *Chem. Lett.* **43**, 199–200.
- Martin, E. E. and Scher, H. D. (2004) Preservation of seawater Sr and Nd isotopes in fossil fish teeth: bad news and good news. *Earth Planet. Sci. Lett.* **220**, 25–39.
- Ohta, J., Yasukawa, K., Machida, S., Fujinaga, K., Nakamura, K., Takaya, Y., Iijima, K., Suzuki, K. and Kato, Y. (2016) Geological factors responsible for REY-rich mud in the western North Pacific Ocean: Implications from mineralogy and grain size distributions. *Geochem. J.* **50**, 591–603.
- Ruttenberg, K. C. and Berner, R. A. (1993) Authigenic apatite formation and burial in sediments from non-upwelling, continental margin environments. *Geochim. Cosmochim. Acta* **57**, 991–1007.
- Talley, L. D. (2007) *Hydrographic Atlas of the World Ocean Circulation Experiment (WOCE). Volume 2: Pacific Ocean* (Sparrow, M., Chapman, P. and Gouldm, J., eds.), International WOCE Project Office, Southampton, U.K., ISBN 0-904175-54-5.

SUPPLEMENTARY MATERIALS

URL (<http://www.terrapub.co.jp/journals/GJ/archives/data/52/MS522.pdf>)
Tables S1 and S2